ATTENUATION OF PROGRAMMED -1 RIBOSOMAL FRAMESHIFTING IN VENEZUELAN EQUINE ENCEPHALITIS VIRUS AS A VACCINE STRATEGY

by

Caitlin Woodson Lehman

A Thesis
Submitted to the
Graduate Faculty
of
George Mason University
in Partial Fulfillment of
The Requirements for the Degree
of
Master of Science
Biology

Committee:

_____ Dr. Kylene Kehn-Hall, Thesis Director

_____ Dr. Monique van Hoek, Committee Member

_____ Dr. Lance Liotta, Committee Member

_____ Dr. Iosif Vaisman, Director, School of Systems Biology

_____ Dr. Donna M. Fox, Associate Dean, Office of Academic Affairs and Special Programs, College of Science

_____ Dr. Peggy Agouris, Dean, College of Science

Date: _____ Fall Semester 2018
George Mason University
Fairfax, VA

Attenuation of Programmed -1 Ribosomal Frameshifting in Venezuelan Equine Encephalitis Virus as a Vaccine Strategy

A Thesis submitted in partial fulfillment of the requirements for the degree of Master of Science at George Mason University

by

Caitlin Woodson Lehman
Bachelor of Science
Virginia Tech, 2010

Director: Kylene Kehn-Hall, Associate Professor
School of Systems Biology

Fall Semester 2018
George Mason University
Fairfax, VA

DEDICATION

This is dedicated to my late grandmother, Jane Holt Woodson. My success is a result of her unconditional love, support, encouragement, and guidance.

ACKNOWLEDGEMENTS

First and most importantly, I would like to thank my thesis director, Dr. Kylene Kehn-Hall, for providing me the opportunity to work in her lab. Her guidance, patience, and flexibility with me during this process has been instrumental in helping me become a scientist that can think critically and produce meaningful data. Her outstanding mentorship has helped me to become a better professional and I know that the qualities and skills she has engrained in me will help me succeed for many years to come. I am honored and ecstatic to continue to work in her lab while I pursue my PhD.

I also would like to thank Dr. Cynthia de la Fuente for being my initial and most impactful mentor. Her patience and/or lack thereof at times helped me to acquire the discipline required to be a good student and scientist. Her knowledge and advice has been invaluable over the years and it was a privilege and honor to work with her. I would also like to thank Dr. Shih-Chao Lin for his willingness to provide support and technical expertise with my experiments, especially *in vivo* experiments. I would also like to thank Dr. Chelsea Pinkham whose unwavering support and encouragement helped keep me sane throughout this academic process.

Many thanks to my committee members, Dr. Monique van Hoek and Dr. Lance Liotta, for their input on this thesis and their support along the way.

Thank you to Dr. Jonathan Dinman and Dr. Joseph Kendra for their work with molecular biology aspects of this project.

Finally, thank you to my husband and family for always encouraging me to pursue my dreams. They have had to make sacrifices to support me in this endeavor and I am forever grateful.

TABLE OF CONTENTS

LIST OF FIGURES

LIST OF ABBREVIATIONS

Animal Biosafety Level 3 ..... ABSL3
Days Post Infection ..... DPI
Dulbecco's Modified Eagle Medium ..... DMEM
Eastern Equine Encephalitis Virus ..... EEEV
Fetal Bovine Serum ..... FBS
Hours Post Infection ..... HPI
Human Immunodeficiency Virus ..... HIV
Multiplicity of Infection ..... MOI
Nonstructural Protein ..... NSP
Open Reading Frame ..... ORF
Quantitative Reverse Polymerase Chain Reaction ..... qRT-PCR
Ribonucleic Acid ..... RNA
Phosphate Buffered Saline ..... PBS
Polymerase Chain Reaction ..... PCR
Plaque Forming Unit ..... PFU
Programmed Ribosomal Frameshifting ..... PRF
Semiliki Forest Virus ..... SFV
Severe Acute Respiratory Syndrome Coronavirus ..... SARS COV
Termination codon readthrough ..... TCR
Trans-frame ..... TF
Venezuelan Equine Encephalitis Virus ..... VEEV
Venezuelan Equine Encephalitis Virus Trinidad Donkey ..... VEEV TrD
Wild type ..... WT
Western Equine Encephalitis Virus ..... WEEV
West Nile Virus ..... WNV

ABSTRACT

ATTENUATION OF PROGRAMMED -1 RIBOSOMAL FRAMESHIFTING IN VENEZUELAN EQUINE ENCEPHALITIS VIRUS AS A VACCINE STRATEGY

Caitlin Woodson Lehman, M.S.

George Mason University, 2018

Thesis Director: Dr. Kylene Kehn-Hall

Venezuelan equine encephalitis virus (VEEV) is a New World alphavirus that is capable of causing significant disease in equines and humans. Moreover, infection with VEEV can be fatal in up to 90% of cases for equines. In humans, while death is rare, infection with VEEV can result in debilitating neurological sequelae. The current vaccines for VEEV are a live-attenuated vaccine (TC-83) and an inactivated form of the vaccine (C-84). However, neither of these are approved by the FDA for human use and only at risk military personnel and laboratorians are vaccinated. We are studying the rational design of VEEV vaccines through mutation of the programmed -1 ribosomal frameshifting (-1 PRF) signal of VEEV. Use of the -1 PRF signal allows production of the viral *trans*-frame protein of VEEV, which is known to play a role in neuropathogenesis. Our lab recently characterized the -1 PRF signals for alphaviruses and results revealed novel -1 PRF stimulatory structures. While disruption of the -1 PRF signal mildly affected VEEV

kinetics in cell culture, it significantly inhibited its pathogenesis in mice challenged subcutaneously or via aerosol. In addition to markedly increased survival, mice exposed to the -1 PRF mutant VEEV (VEEV TrD_{PRFm}) displayed less severe clinical signs and weight loss over the course of infection compared to wild-type (WT) control mice. Serial sacrifice studies indicated mice exposed to VEEV TrD_{PRFm} had either undetectable or reduced levels of virus in the brain, spleen, and serum at all timepoints assayed indicating that dissemination of VEEV TrD_{PRFm} is altered *in vivo*, resulting in less viral replication and overall decreased pathogenesis. Finally, mice vaccinated with VEEV TrD_{PRFm} developed strong neutralizing antibodies and were protected against lethal challenge with aerosolized VEEV TrD. These studies indicate that targeting translational recoding events such as frameshifting is a potential avenue of inquiry for rational vaccine development.

INTRODUCTION

Venezuelan Equine Encephalitis Virus

Background and Significance

Venezuelan equine encephalitis virus (VEEV) is a New World alphavirus that is capable of causing significant disease in equines and humans. VEEV was isolated in Venezuela, as its name implies, from the brain of an infected animal in 1938 (1). Unlike Old World alphaviruses which cause arthritic disease and are endemic to Asia, Europe, Australia, and Africa, New World alphaviruses such as VEEV, eastern equine encephalitis virus (EEEV), and western equine encephalitis virus (WEEV) cause characteristic encephalitic disease and are endemic to the Americas. While in humans death is rare (1%), VEEV infection in equines can result in mortality in 20-80% of cases, affecting thousands of horses each year (1). Humans are infected with VEEV when an infected arthropod vector, typically *Culex* or *Aedes* mosquitoes, takes a blood meal and transmits the virus through the salivary ducts and into the vertebrate host (2). Once infected, humans tend to experience mild to moderate flu-like symptoms including fever, headache, general myalgia and fatigue. If the disease progresses to encephalitis, which occurs in 4-14% of cases, it is accompanied by severe and chronic neurological sequelae (3). Neurological sequelae commonly associated in VEEV survivors is confusion, convulsions, coma, intellectual disability, and behavioral changes, all of which can severely impact the survivors and

caretakers quality of life and result in high financial burden (3,4). Due to the lack of FDA approved therapeutics or vaccines and its history of being weaponized by the former Soviet Union and the United States, it is important to elucidate the mechanisms underlying VEEV infection in vertebrate hosts in the quest to identify suitable countermeasures (5).

Molecular Biology

VEEV is a positive sense, single-stranded RNA virus of the family *Togaviridae*, genus *Alphavirus*. The virus is enveloped and the envelope consists E1 and E2 glycoprotein components creating icosahedral symmetry (3). The genome organization of VEEV contains two open reading frames (Fig. 1A). The first open reading frame encodes for the genomic non-structural proteins (nsP1-4) and the second subgenomic reading frame encodes for up to six proteins: capsid, E3, E2, 6k, *trans*-frame (TF), and E1. The function of nsP1 is mRNA capping which serves to protect the viral RNA from degradation from host cellular nucleases (6,7). nsP2 functions as a protease and cleaves the non-structural polyprotein into its individual components. It also ensures that infectious virions are produced through regulating packaging of the viral genome (8). Meanwhile, nsP3 interacts with host cell machinery to effect viral replication and nsP4 functions as the RNA dependent RNA polymerase (9, 10). The structural protein capsid binds to viral RNA to facilitate assembly of virions (3). The envelope protein E2 facilitates receptor binding and cellular entry via receptor-mediated endocytosis while E1 is a fusion protein which enables fusion of the viral and endosomal membranes (11). The 6K gene is a 6 kilodalton protein that functions in budding and also functions as an ion channel. However, in 2008 it was discovered that due to a frameshifting event that occurs the 6K gene actually yields two

proteins: 6K and TF. The TF protein is present in infectious virions and has been shown to be important for viral dissemination and neuropathogenesis.

During infection of host cells, the E2 glycoprotein interacts with host cell surface receptors and endocytosis ensues allowing the positive-sense RNA genome to be delivered to the cytoplasm where all translation and replication occurs. The virus avoids host cell responses in vertebrates by rapid shutoff of host cell transcription which can be facilitated by nsp2 or capsid (12). Once replication is complete, the virus is assembled into fully mature virions and is released at the plasma membrane.

Programmed Ribosomal Frameshifting

Due to their small genomes, RNA viruses are inherently limited in their coding capacity. To counter this deficit, RNA viruses utilize alternative mechanisms to expand their coding capacity such as alternative splicing, RNA editing, leaky scanning or programmed ribosomal frameshifting (PRF) (13-16). While normally ribosomes strictly follow the reading frame of the mRNA being translated, some viral mRNAs are capable of inducing ribosomes to pause, shift, and adjust reading frame, usually either 1 nucleotide in the 3' direction (+1 PRF) or 1 nucleotide in the 5' direction (-1 PRF) resulting in the synthesis of a protein with an alternative C-terminal peptide sequence (13). The phenomena of frameshifting occurs as a result of three important elements: a seven nucleotide 'slippery site' where the frameshift occurs, a short spacer region, and a downstream stimulatory structure, often a pseudoknot, which provides the kinetic energy required to enable the mRNA to shift one base relative to the ribosome (13, 17). West Nile virus (WNV), human immunodeficiency virus (HIV), severe acute respiratory syndrome coronavirus (SARS-

CoV) and alphaviruses have all been identified as utilizing -1 PRF (13, 16-20)(13, 16-15, 20).

Alphaviruses contain a conserved “slippery site” sequence (U_UUU_UUA) within the 6K gene. Frameshifting that occurs as a result of encountering this sequence, which is during approximately 10-18% of translational events, results in the synthesis of an additional protein with an alternative C-terminal peptide sequence, called the *trans*-frame (TF) (22, 23). Using bioinformatics, alphaviruses were predicted to use -1 PRF and this was confirmed via mass spectrometry for Old World alphaviruses Semliki Forest virus (SFV), Sindbis virus (SINV), and chikungunya virus (CHIKV) (20, 23). It has been shown using SINV that altering the production, size, or sequence of the TF *in vitro* results in reduced levels of SINV release from both mammalian and mosquito cells. Importantly, SINV with a mutated TF protein proved to be less lethal in an SINV neuropathogenic mouse model suggesting that TF plays a critical role in pathogenesis (20). More recently, New World alphaviruses (EEEV, VEEV, and WEEV) were confirmed to induce efficient levels of -1 PRF and these signals were found to be stimulated by tandem-stem loops, not the classic pseudoknot (13). Thus, our research is focused on the development of a TF mutant VEEV to explore the use of -1 PRF attenuation as a general strategy for the rational development of live attenuated vaccines.

Prior studies have suggested that viral −1 PRF signals have evolved to promote frameshifting at very precise rates and that changes in −1 PRF efficiencies have detrimental effects on virus propagation (25, 26). Recently, our lab investigated the importance of −1 PRF on virus propagation in cultured cells by inducing a silent protein-coding change into

the VEEV infectious clones for the TC83 vaccine strain and the highly pathogenic Trinidad Donkey (TrD) strain (27) to create pTC83$_{PRFm}$ and pTrD$_{PRFm}$, respectively (Fig. 1A). The PRF mutant virus was designed with silent nucleotide mutations on the wobble base in the slippery sequence resulting in reduced levels of -1 PRF events (WT -1 PRF occurred ~5%, while the mutant was ~0.3%) which presumably reduces but does not eliminate TF protein production. Meanwhile, the PRF mutant virus still produces capsid, E3, E2, 6K and E1 (Fig. 1B). In contrast, wildtype (WT) virus produces capsid, E3, E2, 6K and E1 the majority of the time, but ~4-6% of the time it switches via frameshifting to produce capsid, E3, E2, and TF (13). Surprisingly, ablation of −1 PRF within the TC83 backbone had minimum effects on virus titers and viral RNA accumulation. However, disruption of the −1 PRF signal within TrD resulted in decreased viral titers (∼1.5 logs) starting at 9 hpi. Viral RNA levels were not affected until later on in the infection (18 hpi) which is consistent with a defect in viral assembly (13). With several substitutions within E2 and E1 between TrD and TC83 (as noted within Materials and Methods), this may indicate that there is less dependence on the −1 PRF signal for the attenuated TC83 strain *in vitro*.

Rationale

Previous studies in which -1 PRF was mutated in flaviviruses revealed that the PRF product is necessary for neuroinvasion and replication in both avian and insect hosts (28, 29). It has also been shown that deleting the 6K gene of Ross River alphavirus results in reduced pathogenesis in mice (30) (28). Moreover, Snyder *et al.* demonstrated that Old World alphavirus SINV is less lethal when the TF is mutated (19). Thus, we aimed to determine if ablation of -1 PRF signal in VEEV-TrD (as shown in Figure 1) affects mouse

survival in a similar manner. We chose to employ VEEV-TrD$_{PRFm}$ since the most significant decreases in viral replication and RNA were observed in the TrD mutant strain compared to the TC83 mutant.

The current vaccines for VEEV are a live-attenuated vaccine (TC-83) and an inactivated form of the vaccine (C-84). TC-83 is a live-attenuated strain derived by serial passaging (83x) of the fully virulent TrD in guinea pig heart cells while C-84 is an inactivated form of TC-83 (31, 32). However, due to vaccine side effects and limited seroconversion rates neither of these are approved by the FDA for general population use and only at risk military personnel and laboratorians are vaccinated. Additionally, TC83 at one time was able to infect mosquitoes and resulted in a vaccine-born outbreak in the 1970s. Subsequently, TC83 was attenuated further and the subgenomic promoter was inactivated with 13 synonymous mutations which prevented it from infecting mosquito cells *in vitro* and *in vivo* (32). Since frameshifting has been demonstrated to impact infectivity and neuroinvasiveness in numerous viruses such as SARS-CoV, West Nile virus, Japanese encephalitis virus, and SINV, we are interested in determining if our TF mutant VEEV (VEEV-TrD$_{PRFm}$) will have similar effects and if it can be used to generate neutralizing antibodies without causing overt illness. Our research will provide valuable insight into whether mutating the -1 PRF in alphaviruses could serve as a feasible option for a live-attenuated vaccine. While live-attenuated vaccines are more cumbersome in terms of the regulatory process, they elicit strong neutralizing antibodies and can provide lifelong protection with just one or two doses. Since VEEV is capable of causing

encephalitis and can also be spread via aerosol in times of warfare, a live-attenuated vaccination method is worthy of exploring.

MATERIALS AND METHODS

Cell Culture

Vero (catalog number CCL-81) cells were obtained from ATCC (Manassas, VA). Cells were cultured in Dulbecco's modified Eagle medium (DMEM) supplemented with 1% L-gluatamine and 10% heat-inactivated fetal bovine serum (FBS) and maintained in a humidified 37ºC incubator with 5% CO_2.

Introducing -1 PRF mutations into infectious VEEV clones

Synonymous substitutions to disrupt the -1 PRF signal in the TrD genome were introduced by overlapping PCR extension, using standard techniques. The silent slippery site mutations consisted of the changes T9964G, T9967C, and A9970G to change the U UUU UUA slippery sites to G UUC UUG within the pV3000 (TrD) plasmid. There are six amino acid changes between the TC83 strain and the TrD strains, and all of these lie within the structural coding region: four in E2 (K7N, H85Y, T120R, V192D, T296I) and one in E1 (L161I) [33,34]. Furthermore, the genome of the V3000 clone of TrD utilized for this study also encodes two additional changes within the E2 (one previously published, N239I [35], and one unpublished, E323G). All plasmid constructs were verified by restriction enzyme digestion and sequencing.

VEEV stocks

Viral stocks were produced by electroporation of *in vitro*-transcribed viral RNA generated from either the pV3000 plasmid (TrD [36]), or the PRF mutant $pV3000_{PRF}$ plasmids. In brief, the viral cDNA was linearized using a restriction enzyme and then purified using a MinElute PCR purification kit (Qiagen) according to the manufacturer's directions. Capped RNAs were synthesized using a MEGAscript kit (Invitrogen) with a 2:1 ratio of cap analog [^{m7}G(5')ppp(5')G;NEB] to GTP and treated with DNase I supplied with the kit. RNA was then isolated with an RNeasy minikit with a second DNase I on-column digestion (Qiagen). The RNA integrity and concentration were determined by gel electrophoresis and determination of the absorbance at 260nm, respectively. *In vitro* transcribed viral RNAs were electroporated into BHK-J cells utilizing g a 2-mm-gap cuvette (model BTXECM 630 exponential decay wave electroporator; Harvard Apparatus, Holliston, MA). After trypsination, cells were washed twice and resuspended in cold Dulbecco's phosphate-buffered saline without Ca^{2+} and Mg^{2+} (D-PBS; RNase-free) at 1.25 x 10^7 cells/ml. An aliquot of the cell suspension (400 µl) was mixed with 1 µg of RNA transcripts, placed into the cuvette, and pulsed once at 860 V, a 25-µF capacitance, and a 950 Ω resistance. Cells were allowed to recover for 5 min at room temperature and resuspended in complete minimal essential medium (MEM; Gibco Invitrogen). Cells from three replicate electroporations were plated in three 75-cm2 culture flasks for virus production. On the next day (~12 h post electroporation [hpe]), transfection medium was replaced with fresh MEM. Medium supernatants were harvested at several time points, pooled, and stored at 4ºC. After the last collection, supernatants were then filtered (pore

size, 0.2 μm), aliquoted, and stored at -80ºC. Viral titers were determined by plaque assay on Vero cells.

Plaque Assay

Vero cells were plated at $2.5x10^5$ cells per well in 12-well plates and allowed to incubate overnight at 37°C and 5% CO_2. The following day, Vero cells were infected with dilutions of the supernatants collected. Supernatants were serial diluted 1:10 in triplicates from 10^{-1} to 10^{-8} in complete DMEM. Vero cells were infected with 200 uL of each serial dilution for 1 hour. After infection, a 1-mL overlay of a 1:1 solution of 0.6% agarose in diH2O and 2x EMEM supplemented with 5% FBS, 1% L-glutamine, 1% penicillin/streptomycin, 1% non-essential amino acids, and 1% sodium pyruvate was added to the cells. The cells were incubated at 37°C and 5% CO_2 for 48 hours. After 48 hours, the cells were fixed using 10% formaldehyde overnight at room temperature. Following fixation, the formaldehyde and agar plugs were discarded. The cell monolayers were stained with a solution of 1% crystal violet and 20% methanol to visualize plaques. Plaques were counted and the averages from triplicates were taken. Dilutions with less than 10 or more than 100 plaques were discounted. The viral titer (pfu/mL) was calculated by the average of the triplicates x dilution factor (5) x dilution.

Animal experiments

For the initial study, 6- to 8-week old female BALB/c mice were obtained from Envigo Laboratories and allowed to acclimate. Groups of 35 mice were infected with VEEV TrD or VEEV TrD_{PRFm} using Biaera's AeroMP system, a whole-body chamber, and a three-jet

Collison nebulizer. They were exposed to 1×10^5 PFU/ml of VEEV TrD or VEEV TrD_{PRFm} for 10 min followed by a 5 min air purge. For the nebulizer, virus was diluted to the appropriate concentration in Hanks' balanced salt solution (HBSS) plus 1% FBS for a total of 10 mL. Alternatively, the All Glass Impinger sampler which was used to back titrate the exposed dose was prepared the same as above, without virus. Ten animals from each group were observed for survival over the course of 21 days. Five animals from each group were euthanized on days 2, 4, 6, 8, and 10 postinfection to determine the kinetics of disease in the mouse system. Serum, spleen, and brain were collected from each animal. Organs were homogenized using an Omni Bead Ruptor 4 (Omni International) and then centrifuged at 14,000 rpm for 5 min. The supernatants were analyzed by plaque assays to determine viral titers. Whole blood samples were collected via cardiac puncture and were placed into serum separator tubes (Sarstedt) and then centrifuged at 14,000 rpm for 5 min. As with the organ samples, the serum supernatant was collected and analyzed by plaque assay.

For the vaccination study, 6- to 8- week old female BALB/c mice were obtained from Envigo Laboratories and were allowed to acclimate prior to starting the study. Three days prior to starting the study, all mice underwent subcutaneous temperature transponder (BioMedic Data Systems) implantation. Throughout the study, the mice were weighed daily, scored for clinical symptoms, and body temperature was recorded. On day 0 mice were vaccinated with either 10^3 or 10^4 VEEV TrD_{PRFm} via subcutaneous injection. On day 28 post-vaccination, blood was collected from each mouse via the facial vein. Serum was analyzed for neutralizing antibodies against VEEV TrD using the plaque reduction

neutralizing test (PRNT, described below). Mice were then exposed to virulent VEEV-TrD via aerosol exposure as described above and followed for survival.

All VEEV TrD and VEEV TrD_{PRFm} experiments were performed in animal biosafety level 3 (ABSL-3) facilities, in accordance with the National Research Council's *Guide for the Care and Use of Laboratory Animals* (37) and under George Mason University IACUC protocol number 0331.

PRNT Assay

A PRNT assay was performed to measure the amount of VEEV-specific neutralizing antibodies in mouse sera. Briefly, VEEV TrD was added to twofold serially diluted sera at a concentration of 80 pfu per well. VEEV E2 antibody (BEI Resources, Manassas, VA) was used as a positive control. Vero cells were infected using the diluted sera and virus mixture and were incubated for 1h at 37°C. Following infection, a 1-mL overlay of a 1:1 solution of 0.6% agarose in diH2O and 2x EMEM supplemented with 5% FBS, 1% L-glutamine, 1% penicillin/streptomycin, 1% non-essential amino acids, and 1% sodium pyruvate was added to the cells. The cells were incubated at 37°C and 5% CO_2 for 48 hours. After 48 hours, the cells were fixed using 10% formaldehyde overnight at room temperature. Following fixation, the formaldehyde and agar plugs were discarded. The cell monolayers were stained with a solution of 1% crystal violet and 20% methanol to visualize plaques. Percent neutralization was calculated as: [(number of VEEV plaque per well without anti-VEEV serum) - (number of VEEV plaque per well of diluted anti-VEEV serum)/(number of VEEV plaque per well without anti-VEEV serum) x 100]. Neutralizing

antibody titers were expressed as the reciprocal of the highest dilution of serum that neutralized 80% of VEEV.

Statistical Analysis

Statistical analysis for viral kinetics was performed using Prism, version 6, software (Graphpad). Kaplan Meyer survival plot (also in Prism) was used to determine statistical significance of survival studies.

RESULTS

Ablation of -1 PRF strongly attenuates VEEV pathogenesis

Prior studies in which −1 PRF was ablated in flaviviruses revealed that the NS1′ frameshift PRF product is required for neuroinvasion and replication in both avian and insect hosts (28, 38). Similarly, deletion of the 6K gene reduced the pathogenesis of the Ross River alphavirus in mice (39). Likewise, deletion of 6K in CHIKV resulted in drastically reduced clinically symptoms in a mouse model and also elicited protection from future CHIKV challenge (40). To determine the importance of the −1 PRF signal for VEEV pathogenesis, six-to-eight week old BALB/c mice were exposed to 1×10^5 pfu/ml of VEEV TrD or VEEV TrD_{PRFm} for 10 min via the aerosol route. Prior to exposure, all mice were weighed to establish a baseline average weight to be used to calculate the percent change in weight for the duration of the study. Two groups of mice were followed for 21 days in order to assess survival, while others were sacrificed over the course of infection to assess viral kinetics *in vivo*. All mice were weighed and examined for clinical signs at least once daily. Clinical symptoms associated with our established VEEV mouse model are weight loss (>30%), ruffled fur, hunched posture, closed eyes, lethargy, and rear-limb paralysis. The typical timeframe in our established model for VEEV associated clinical symptoms are 2-14 days post-infection (dpi) where the animals will either succumb to infection or recover from infection and survive which

is consistent with others published model data (41). Mice were scored using four categories: appearance, mobility, attitude, and body condition. For appearance, scoring parameters were defined as: (0) smooth coat, bright eyes; (1) slightly scruffy and/or slightly hunched at rest; (2) scruffy and/or hunched at rest; (3) very scruffy and/or hunched, mild eye crust; or (4) very scruffy and/or very hunched, closed eyes. For mobility, scoring parameters were defined as: (0) active, foraging and exploring cage; (1) walking, less active; (2) slow movement; (3) no movement; or (4) unresponsive. For attitude, scoring parameters were defined as: (0) alert; (1) mildly lethargic; (2) lethargic; or (3) unaware. For body condition, scoring parameters were defined as: (0) obese or normal; (1) underconditioned; or (3) emaciated. Scores for each category were tallied for a total score which was used to determine how severe symptoms were and if additional monitoring or euthanasia was required. Total score parameters were defined as: (0-5) normal once daily monitoring, (6-10) twice daily monitoring, 8 hours apart, and (≥11) were considered moribund and were immediately and humanely euthanized using CO_2. To ensure the utmost welfare of the animals, all mice were provided additional nesting materials, moist feed, and feed on the floor of the cage throughout the study.

Kaplan-Meier survival analysis shows that ablation of −1 PRF had a strong negative effect on VEEV-induced mortality (Fig. 2A). VEEV TrD-infected mice succumbed to infection beginning at 8 dpi, with all mice succumbing by 13 dpi. In contrast, 70% of VEEV TrD_{PRFm}-infected mice survived the infection. Weight loss (Fig. 2B) and clinical symptoms of disease (Fig. 2C) were less severe and delayed in VEEV TrD_{PRFm}-infected mice compared to VEEV TrD-infected mice. Mice infected with VEEV

TrD began losing weight as early as 1 dpi and continued to rapidly lose weight (up to 50% of initial body weight) until death. Conversely, mice infected with VEEV TrD_{PRFm} did not show signs of weight loss until 6 dpi with weight loss peaking (approximately 20% of initial body weight) 13 dpi and returning to baseline by 21 dpi.

As expected, clinical symptoms appeared 2 dpi in VEEV TrD-infected mice and gradually increased in severity until death. From 2-6 dpi these mice were scruffy, less active, and losing weight. Upon day 6 the clinical symptoms were more pronounced with the animals displaying a scruffy appearance, hunched posture, lethargy, and significant weight loss. Beginning day 8, VEEV TrD-infected mice displayed clinical signs of morbidity as defined by our established scoring parameters and were euthanized upon reaching a moribund state. Bilateral rear limb paralysis was observed in 30% of VEEV TrD-infected mice which was not unexpected since VEEV infection is known to induce altered gait in equines and we have previously observed rear limb paralysis in developing our VEEV-TrD mouse model (42).

Remarkably, VEEV TrD_{PRFm}-infected mice appeared unaffected by the infection until 8 dpi. Upon onset of clinical symptoms, 70% of mice had their condition remain stable, with the exception of weight loss, and began to improve within 6 days or sooner of symptom onset. Two mice succumbed to infection. However, it should be noted that these animals did not display severe signs of clinical disease but were euthanized due to unilateral rear limb paralysis. While those two animals may have ultimately survived the infection, we chose to euthanize them to ensure they did not suffer from unnecessary stress induced by one limb being immobile and potentially interfering with ease of access

to food and water. Additionally, one animal was euthanized due to self-mutilation which could be attributed to the inherent neuropathogenesis associated with VEEV infection.

In parallel experiments, virus titers in the serum, spleens, and brains of infected mice were monitored every 2 days for 10 days total. In all of the VEEV TrD-infected mice, virus was detected in the blood and spleen early after infection (2 and 4 dpi) and cleared by 6 dpi (Fig 3). In contrast, following infection with VEEV TrD_{PRFm}, virus was detectable in the blood and spleen in only 50% of the mice at 2 dpi and in only 60% of the mice at 4 dpi. Virus was also detected in the spleen at 6 dpi in 80% of the VEEV TrD_{PRFm}-infected mice. Plaque assays of brains revealed the presence of high levels of virus in the VEEV TrD-infected mice at all time points tested. In contrast, virus was not detectable in the VEEV TrD_{PRFm}-infected mice until 4 dpi and was cleared in 80% of those mice by 10 dpi. It should be noted that the 3 mice that died from VEEV TrD_{PRFm} infection succumbed on Days 9, 10, and 14 post-infection thus our serial sacrifice studies only represent a snapshot of viral kinetics in vivo in the later timepoints. Additionally, we presume that the VEEV TrD-infected mice from the Day 10 timepoint would have succumbed to infection due to the presence of severe clinical symptoms, high viral load in the brain, and also having 100% lethality in the alongside survival study. Overall, these results indicate that the dissemination of VEEV TrD_{PRFm} is altered *in vivo*, resulting in less viral replication within the brain and overall decreased pathogenesis.

Vaccination with $VEEV_{PRFm}$ produces strong neutralizing antibodies

Since we observed altered viral expression *in vivo*, particularly within the brain, we sought to determine if exposure to lower doses of the mutant virus administered subcutaneously could elicit the development of neutralizing antibodies against VEEV without causing overt disease. To this end, six-to-eight week old BALB/c mice were inoculated subcutaneously with $VEEV_{PRFm}$ at $1x10^3$ (n=10) or $1x10^4$ (n=10) pfu/mouse. VEEV-TC83 was used as a positive control (n=5) at a dose of $1x10^5$ pfu. Alternatively, PBS was used as vehicle control (n=5). Upon inoculation, all mice were monitored at least once daily, weighed daily, and were scored for clinical symptoms associated with VEEV infection as described in the section above. In addition to those parameters, we also recorded internal body temperature by subcutaneously implanting a temperature transponder chip (BioMedic Data Systems) in each mouse prior to starting the study which allowed us to record body temperature without physically restraining the mouse which could induce unnecessary stress not associated with VEEV infection and result in inaccurate temperature readings (41).

Mice receiving the vehicle control and TC-83 appeared normal and were bright, alert, and responsive through Day 28. Mice receiving $VEEV_{PRFm}$ appeared normal the first two days post-inoculation. However, upon day 3 both groups of $VEEV_{PRFm}$ mice started losing weight and began to appear slightly scruffy (Fig. 4 and 5). The most common clinical symptoms observed in these mice were ruffled fur and reduced activity with clinical signs appearing and waning over time back to normal within 7-14 days (Fig 8). While approximately 10-20% weight loss was observed in $VEEV_{PRFm}$ groups, weight loss was not as significant as typically seen with wild-type VEEV TrD infections where

mice can lose more than 30% of their initial starting weight. Three mice succumbed to illness in the $VEEV_{PRFm}$ $1x10^4$ pfu group (on days 11, 13, and 18 post vaccination) and one mouse died in the $1x10^3$ pfu group (day 8 post vaccination) (Fig.6).

On day 28, blood was collected from surviving mice in all groups and serum was tested for neutralizing antibodies against VEEV via plaque reduction neutralization test (PRNT). As expected, vehicle control mice had no detectable antibodies against VEEV (Fig. 7). Remarkably, mice vaccinated with $VEEV_{PRFm}$ elicited a robust amount of neutralizing antibodies, approximately 0.5-1 log higher to that of those vaccinated with TC83. These results suggest that while exposure to $VEEV_{PRFm}$ at these doses is capable of inducing mild clinical symptoms and in some instances death, exposure to $VEEV_{PRFm}$ is sufficient to develop strong neutralizing antibodies against VEEV which could ultimately provide protection against lethal challenge doses.

Vaccination with $VEEV_{PRFm}$ protects mice from subsequent challenge with VEEV TrD

On day 29 post vaccination with PBS, TC83, or $VEEV_{PRFm}$ all remaining mice were exposed to fully virulent VEEV-TrD at a dose of $1x10^5$ pfu/ml via aerosol route. Prior to exposure all mice appeared normal and were bright, alert, and responsive. After exposure, all mice were followed for survival and clinical symptoms, body weight, and body temperature were monitored at least daily. As anticipated, mice inoculated with PBS vehicle control displayed clinical signs of VEEV infection within 2 dpi (Fig. 5). Clinical symptoms increased in severity until ultimately 4 out of 5 mice succumbed to

infection on days 6-7 post aerosol challenge. Mice in the vehicle control group exhibited weight loss (approximately 30%) as typically seen with our VEEV mouse model (Fig. 4). Additionally, body temperatures in the vehicle control group increased for the first three days indicating that the immune system was actively trying to fight off the infection (Fig 9). However, the viral infection succeeded in overwhelming the host immune response and body temperatures began to drop significantly before death. One mouse from the vehicle cohort exhibited clinical signs of illness but ultimately survived the post-vaccination infection with virulent VEEV TrD (Fig. 8). This is likely attributable to these mice aging over the experiment to approximately 11-12 weeks old and having a more fully developed and mature immune system (43) while our established VEEV TrD aerosol exposure dose has been optimized for 6 week old BALB/c mice. All mice exposed to either TC83 or $VEEV_{PRFm}$ were protected against clinical disease and morbidity associated with fully virulent VEEV with no clinical symptoms being observed throughout the 12 days they were followed after challenge. There was a slight increase in all group temperatures on day 29 (Fig. 9), however that is likely due to the stress induced from being transferred from their home cages to the aerosol chamber and back and/or the viral challenge itself. Both TC83 and $VEEV_{PRFm}$ groups had normal temperatures throughout the 12 days they were followed after challenge. Overall, results from this study suggest $VEEV_{PRFm}$ is capable of eliciting strong neutralizing antibodies and protection against subsequent infection if the mice survive the vaccination, indicating that $VEEV_{PRFm}$ is worthy of further exploration as a platform for rational vaccine development.

FIGURES

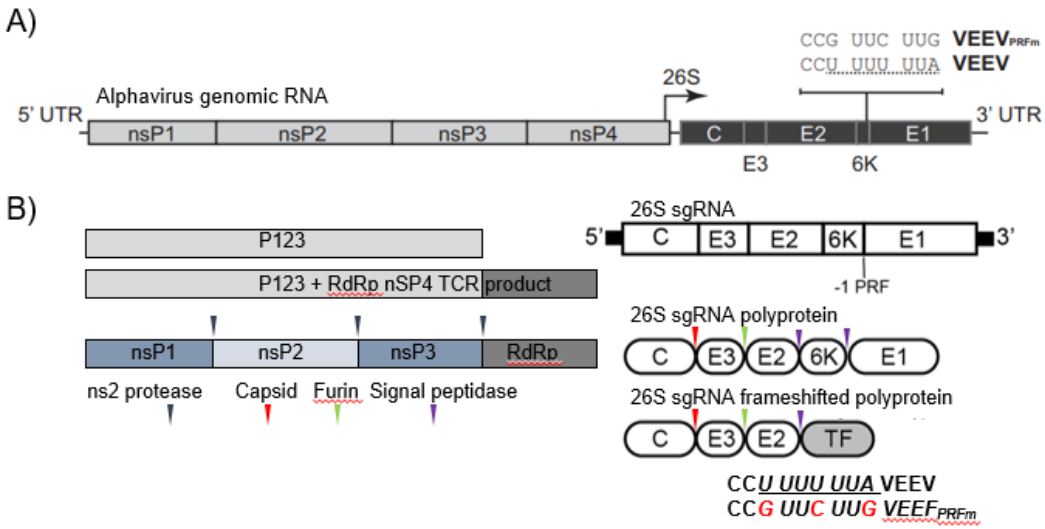

Figure 1
Map of VEEV genome and translational products. (A) Schematic diagram indicating silent coding nucleotide substitutions ablating the −1 PRF signal in the VEEV TrD infectious clone (VEEV$_{PRFm}$). (B) Expanded schematic of the translational products. The 26S sgRNA polyprotein represents the wild-type proteins produced during translation. The 26S sgRNA frameshifted polyprotein represents the *trans*-frame protein being produced as a result of frameshifting, which occurs in 10-18% of translational events. The wild-type VEEV -1 PRF slippery-site is underlined while the VEEV$_{PRFm}$ silent coding changes are shown in red.

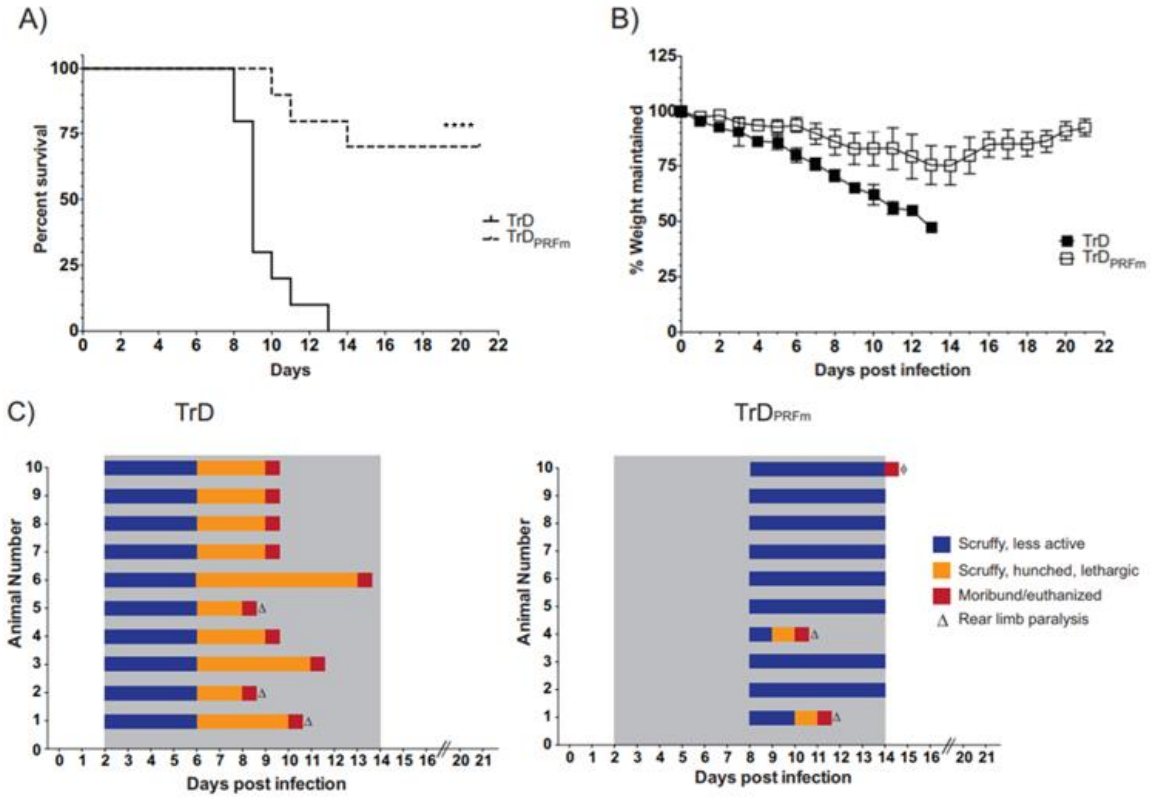

Figure 2

Ablation of -1 PRF strongly attenuates VEEV pathogenesis. (A) BALB/c mice were infected with VEEV TrD or VEEV TrD_{PRFm} by aerosol exposure. Animals were monitored for 21 days postchallenge, and survival curves were determined. The data plotted represent those for 10 animals per group. (B) Mice were monitored for weight loss daily over 21 days. The percentage of weight maintained (relative to the starting weight) was determined. The data plotted represent the mean values and standard deviations for 10 animals per group. (C) Mice were also monitored at least daily for clinical symptoms of disease over 21 days. Data are plotted per animal per day. The gray shaded area indicates the time frame when clinical disease was observed in VEEV TrD-infected mice. ϕ, one animal had to be euthanized due to self-mutilation. Necropsy indicated no signs of disease in this mouse. **** p-value <0.0001

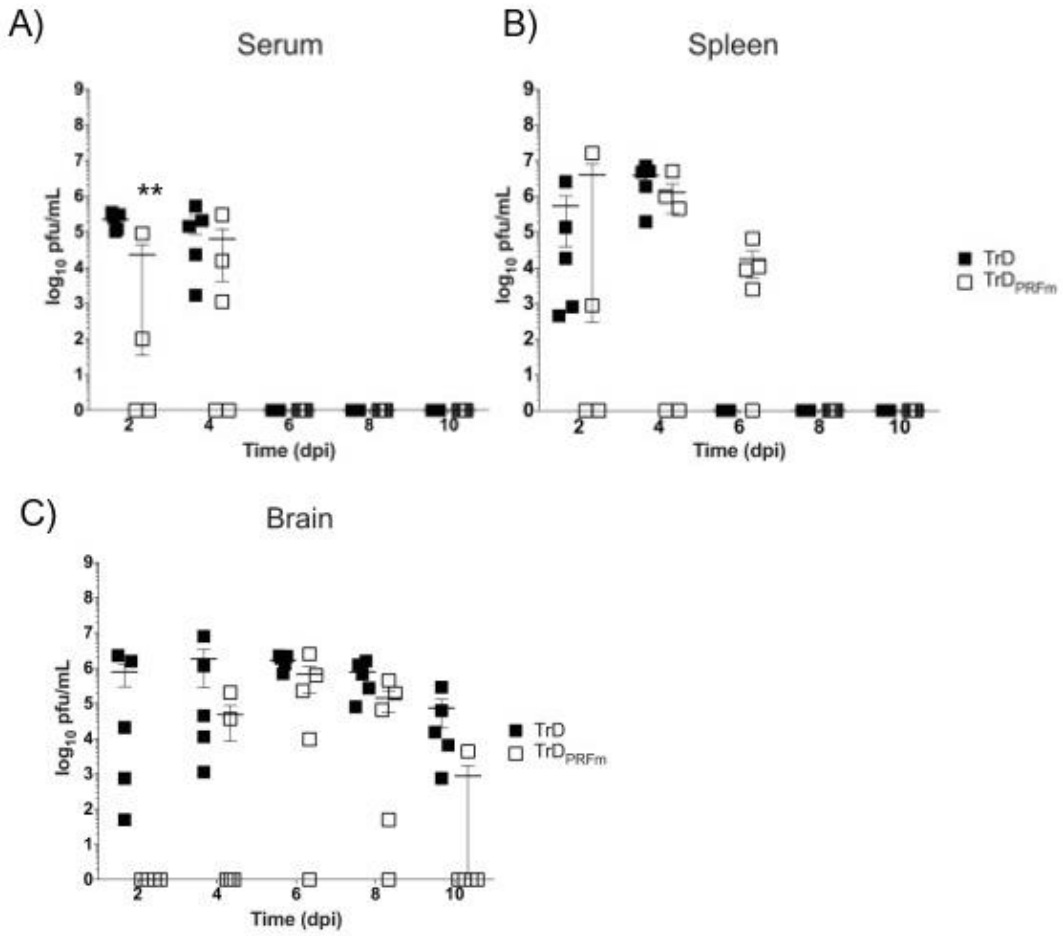

Figure 3

Ablation of -1 PRF results in altered viral kinetics compared to wild-type. Mice were infected as described in Figure 2 and were sacrificed at 2, 4, 6, 8, and 10 dpi. (A)Serum, (B) spleen, and (C) brain were harvested and viral titers were determined by plaque assays. The data plotted represent means and standard errors of the means for five animals per condition. Filled and open squares, VEEV TrD and VEEV TrD_{PRFm}, respectively. Samples without detectable plaques were plotted as 1 PFU/ml. **p<0.01

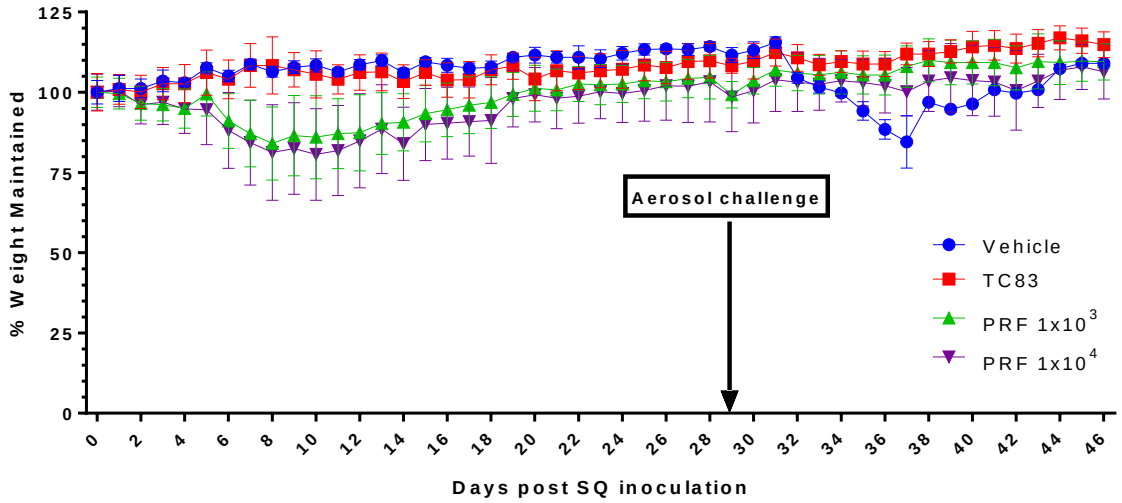

Figure 4

Percent weight maintained post subcutaneous inoculation. Each day throughout the entire study body weight was assessed and compared to the average initial starting weight for each group. This figure represents the mean with standard deviation for each groups average percent weight lost or gained for each day of the experiment. Blue line represents vehicle, red line represents TC83 $1x10^5$ pfu, green line represents VEEV TrD_{PRFm} $1x10^3$ pfu, and purple line represents VEEV TrD_{PRFm} $1x10^4$ pfu. Day 29 represents when surviving vaccinated mice were exposed to fully virulent aerosolized VEEV TrD.

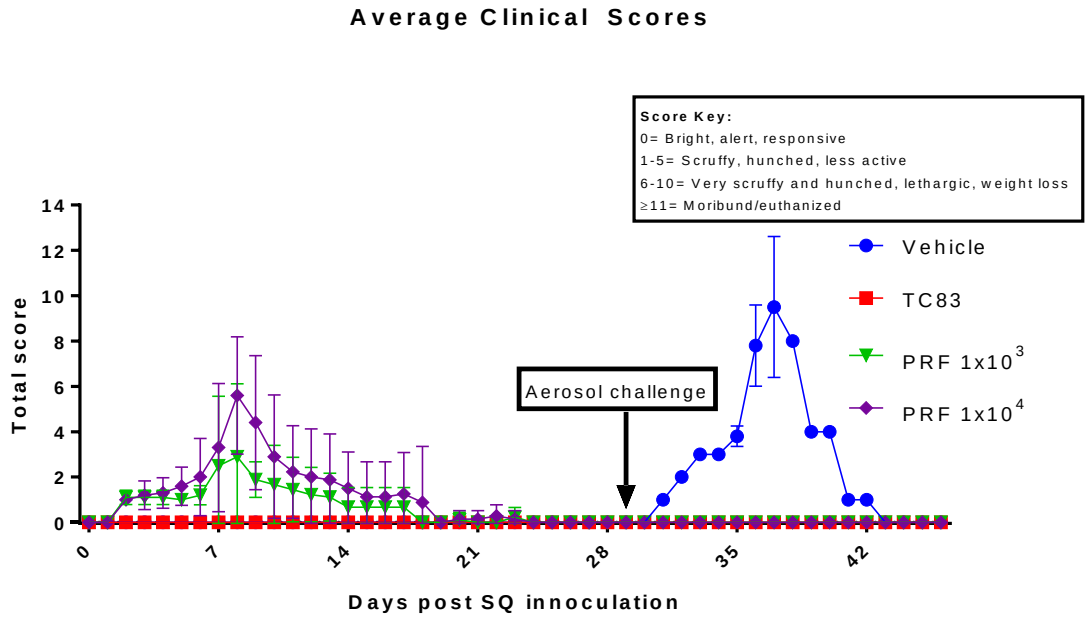

Figure 5

Average clinical scores for each group. Each day throughout the entire study clinical symptoms were recorded and scored according to our established VEEV mouse model clinical scoring parameters as described in the Results section. This figure represents the mean with standard deviation for each groups average clinical score for each day of the experiment. Blue line represents vehicle, red line represents TC83 $1x10^5$ pfu, green line represents VEEV TrD_{PRFm} $1x10^3$ pfu, and purple line represents VEEV TrD_{PRFm} $1x10^4$ pfu. Day 29 represents when surviving vaccinated mice were exposed to fully virulent aerosolized VEEV TrD.

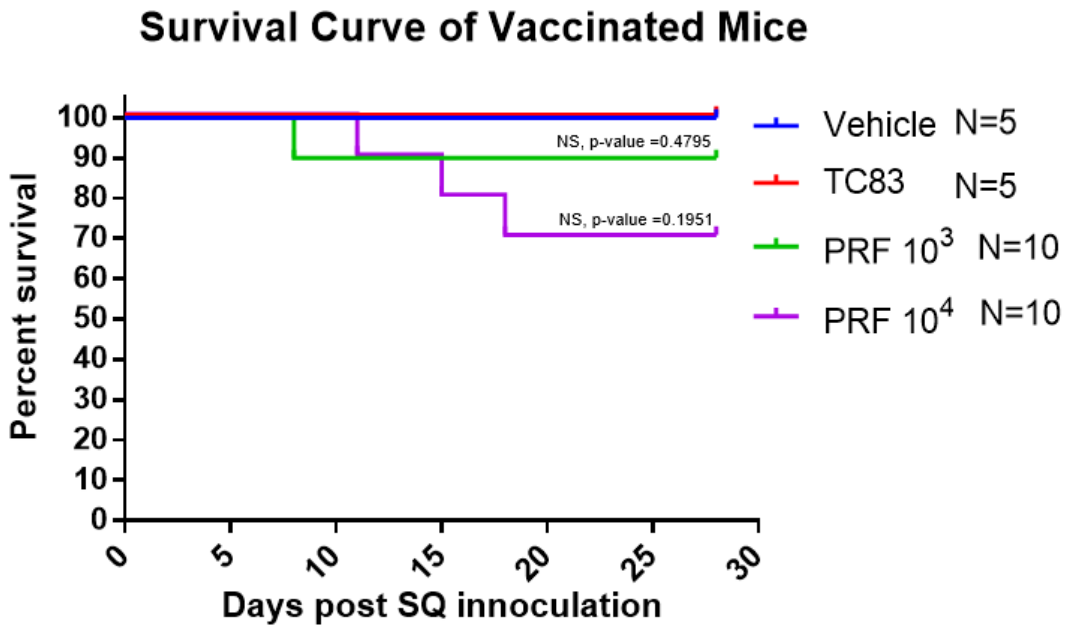

Figure 6

Survival curve of mice vaccinated with VEEV TrD$_{PRFm}$. BALB/c mice were inoculated with vehicle control (PBS) (n=5), TC83 (n=5), or two doses of VEEV TrD$_{PRFm}$ (n=10) via subcutaneous injection. Animals were monitored for 28 days following inoculation and survival curves were determined. Blue line represent vehicle, red line represents TC83 $1x10^5$ pfu, green line represents VEEV TrD$_{PRFm}$ $1x10^3$ pfu, and purple line represents VEEV TrD$_{PRFm}$ $1x10^4$ pfu.

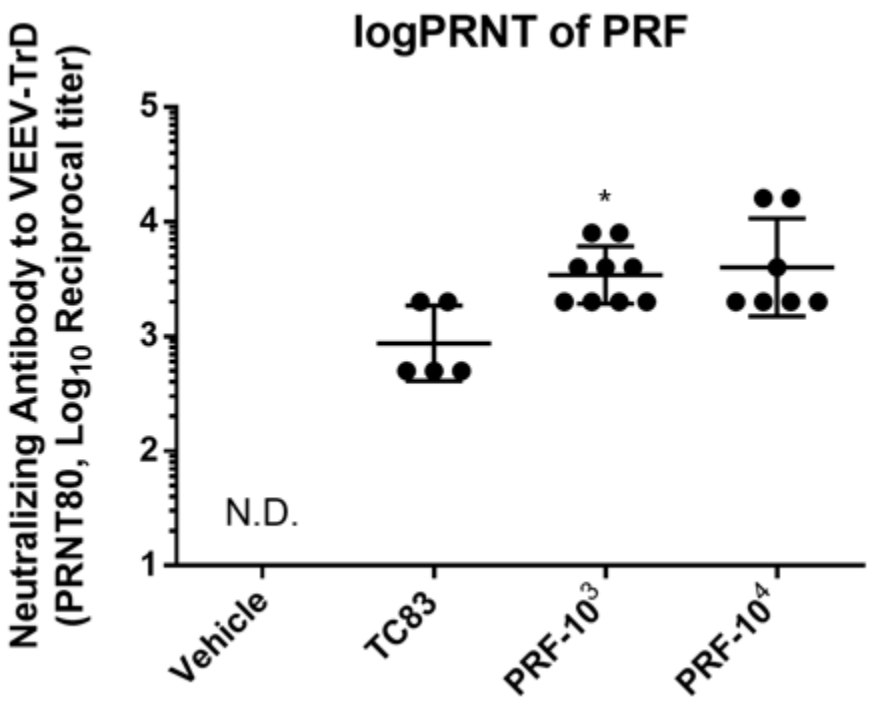

Figure 7

Mice vaccinated with VEEV TrD$_{PRFm}$ produce strong neutralizing antibodies. Serum samples collected at day 28 post-vaccination were analyzed to determine neutralizing antibody levels via $PRNT_{80}$ assay. Vehicle (n=5), TC83 (n=5), $VEEV_{PRFm}$ $1x10^3$ pfu (n=9), $VEEV_{PRFm}$ $1x10^4$ pfu (n=7). *p-value <0.05 compared to TC83

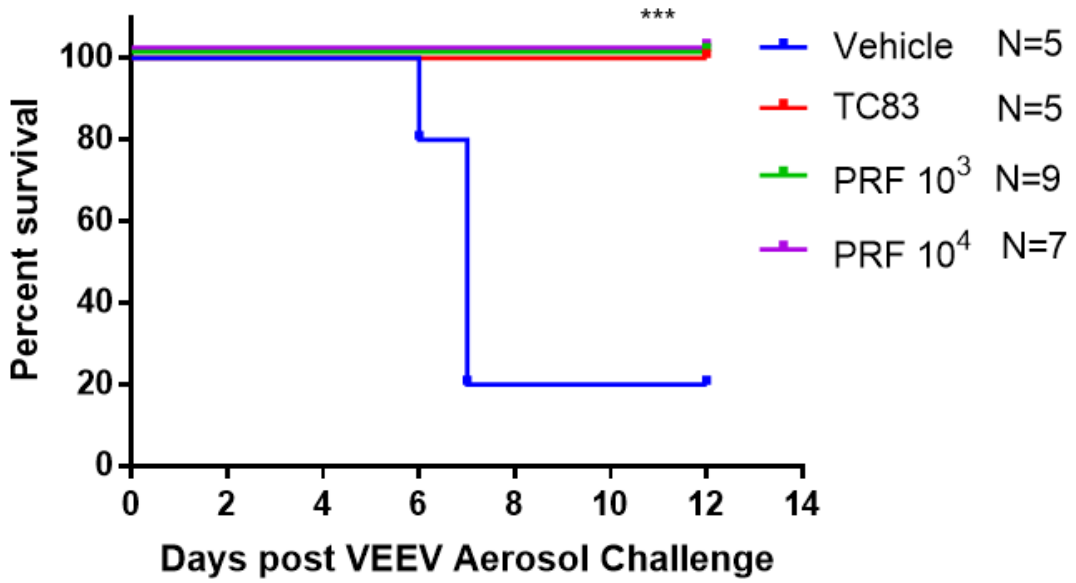

Figure 8

Survival curve of vaccinated post aerosol challenge with fully virulent VEEV TrD. On day 29, the remaining mice from each group were exposed to fully virulent VEEV TrD via aerosol route. Animals were monitored for 12 days post challenge and survival curves were determined. Blue line represent vehicle (n=5), red line represents TC83 $1x10^5$ pfu (n=5), green line represents VEEV TrD_{PRFm} $1x10^3$ pfu (n=9), and purple line represents VEEV TrD_{PRFm} $1x10^4$ pfu (n=7). *** p-value <0.001

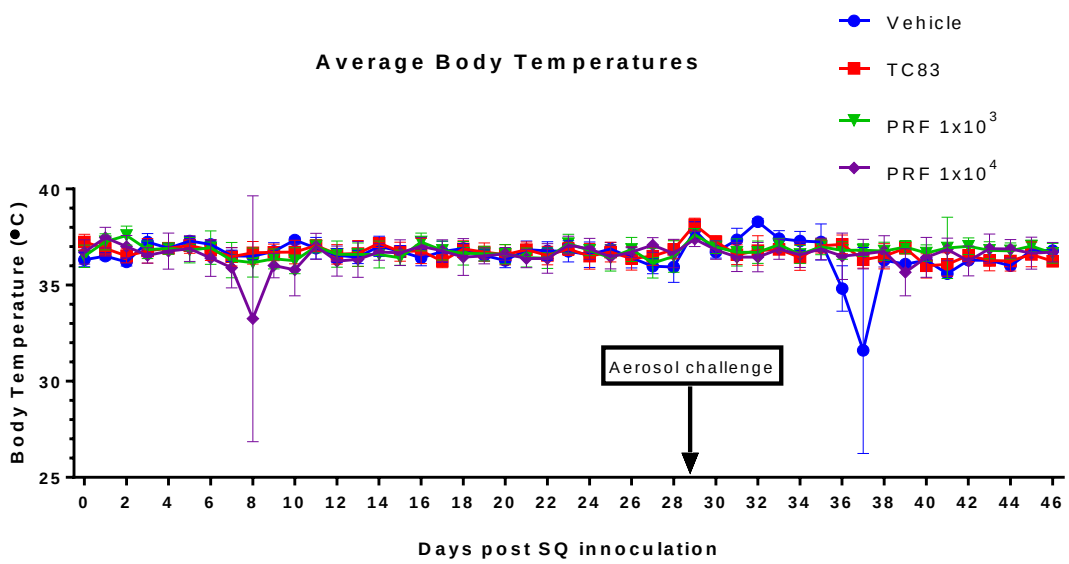

Figure 9

Average body temperatures (°C) for each group. Each animal had their body temperature recorded each day throughout the entire study. Blue line represents vehicle, red line represents TC83 $1x10^5$ pfu, green line represents VEEV TrD_{PRFm} $1x10^3$ pfu, and purple line represents VEEV TrD_{PRFm} $1x10^4$ pfu. Day 29 represents when surviving vaccinated mice were exposed to fully virulent aerosolized VEEV TrD.

DISCUSSION

Programmed −1 ribosomal frameshifting was first discovered in retroviruses, where it directs the synthesis of Gag-Pol polyproteins (44). Subsequent studies using retroviruses (45) and totiviruses (46) demonstrated that changes in −1 PRF efficiency affect virus production. From this, a bioeconomics model emerged in which −1 PRF rates are optimized to maximize virus particle assembly by ensuring the synthesis of the correct stoichiometric ratios of the structural Gag-derived proteins to the enzymes encoded by the Pol open reading frame (ORF) (reviewed in reference 26). These findings engendered interest in targeting −1 PRF for antiviral therapeutics (reviewed in reference 47). In parallel, early studies also examined −1 PRF signals in virus families where they do not occur between ORFs encoding structural and enzymatic ORFs, e.g., in coronaviruses and luteoviruses. The finding that the barley yellow dwarf virus uses −1 PRF as a developmental switch from the initial translation of nonstructural proteins to the translation of proteins involved in viral genome replication represented an expansion of our understanding of the utility of this molecular mechanism (48). Similarly, research in coronaviruses revealed that −1 PRF also serves as a switch, in this case, from expression of immediate early nonstructural proteins that are implicated in modulating the innate immune response to the next developmental step of the viral program, expression of viral replication machinery (reviewed in references 49 and 50) Nonetheless, alteration of −1 PRF efficiency in SARS-

CoV severely impacted its infectivity in tissue culture, reinforcing the idea of −1 PRF as an antiviral therapeutic target (51). In flaviviruses, the viral positive-strand RNA genome encodes a single ORF in which the structural proteins are encoded by the 5′ third of the genome and the 3′ two-thirds encodes the nonstructural proteins. In these viruses, the location of the −1 PRF signal in the first nonstructural gene (NS1) has been proposed to ensure the production of large amounts of structural proteins for virus particle assembly and smaller amounts of the nonstructural proteins (52). Interestingly, lower rates of −1 PRF correlate with decreased pathogenicity in West Nile virus (53), and production of the NS1′ frameshift product is critical for neuroinvasiveness in West Nile and Japanese encephalitis viruses (28, 53). In these viruses, the NS1′ protein is thought to be important for virion assembly (28, 54). Additionally, −1 PRF has now been demonstrated to be used to control the expression of a large fraction of cellular genes in eukaryotes by functioning to control mRNA stability (reviewed in reference 55). Thus, we suggest that −1 PRF is an ancient, basic biological regulatory mechanism that has been evolutionarily selected for numerous end uses.

While alphaviruses are related to flaviviruses, alphavirus genomes are arranged such that the nonstructural proteins are located in the 5′ ORF, while the structural protein genes are in a separate 3′ ORF and are expressed from the 26S subgenomic RNA (Fig. 1A). In alphaviruses, production of the 8.4-kDa TF protein may have two consequences. First, because E1 is a structural protein, −1 PRF may play a role in virion assembly by controlling E1 expression levels, and thus, altered E1 production could negatively interfere with virion assembly (20, 56). Our previous data partially support this model, as ablation of the −1

PRF signal resulted in decreased virion production/release *in vitro* (13). This small decrease in virion production may provide just enough of a difference to enable the host to mount an effective immune response, as evidenced by the longer viral residence times of TrD_{PRFm} in the spleen (Fig. 3). Future studies in our lab will be designed to quantify E1 production levels between the WT and TrD_{PRFm} viruses. Alternatively, the TF protein itself may have a biological role separate from viral particle assembly. This is supported by the observation that −1 PRF inhibition attenuated VEEV pathogenicity and altered viral spread in mice. Consistent with the information on the flavivirus NS1′ protein in the literature, the observation that the TrD_{PRFm} virus promoted decreased viral titers in the brains of infected mice suggests that the VEEV TF protein may be important for passage through the blood-brain barrier and/or for neuroinvasiveness (20, 28, 53). It is important to note that these two options are not mutually exclusive, in that decreased TF protein expression and the accompanying increase in E1 levels may influence viral assembly/release while at the same time impact an as of yet unidentified role of the TF protein. In addition to quantifying levels of E1 between the mutant and WT virus, future studies quantifying the amount of TF produced is required. Furthermore, there have been no studies to date examining the interactions between the TF protein and other viral or cellular proteins. Such analyses would lend great insight into the role of the TF protein and will be emphasized in our future research.

The development of VEEV as a biological weapon in the United States and former USSR and a documented history of over 150 cases of serious laboratory infections with VEEV (1) led to it being included as a select agent by the government of the United States

of America (http://www.selectagents.gov/SelectAgentsandToxinsList.html). As noted above, the FDA has not approved any vaccines or therapeutics for the equine encephalitis viruses for use in humans. The attenuated vaccine strain, TC83, was generated in the early 1960s by serially passing VEEV 83 times in guinea pig heart cells (33). TC83 poses a high risk for reversion due to the fact that it harbors only two attenuating mutations, one in the 5' UTR (nucleotide position 3) and the other in the E2 glycoprotein open reading frame (amino acid position 120) (25, 31) and can also be transmitted by mosquito vectors (57). Because of these risks, coupled with its demonstrated ability to cause mild to severe flu-like symptoms in approximately 25% of volunteers and the fact that it promoted seroconversion in only 80% of volunteers (58) TC83 has only limited utility for use in humans, and its use is restricted to laboratory personnel and members of the military at risk of contracting an infection with the virus (59). More recent live attenuated vaccine candidates are based on the VEEV TrD infectious clone used in the current study. These include clones with insertion of specific point mutations or a mutation in the PE2 cleavage signal combined with a mutation that rescues E1 gene function. The resulting V3526 strain is safe and immunogenic in nonhuman primates and mice and has a lower risk for mosquito transmission (reviewed in reference 59).

In the current study, we demonstrate that VEEV TrD_{PRFm} is attenuated for lethality compared to the WT virus, from 100% lethality in WT to 30% lethality in TrD_{PRFm} 10^4 and 10% lethality with TrD_{PRFm} 10^3. In addition, viral dissemination was reduced *in vivo* with TrD_{PRFm}. Mice that survived vaccination with the PRF mutant virus had strong levels of neutralizing antibody and all survived subsequent challenge with fully virulent TrD

challenge. However, it is important to note that additional improvements in experimental design must be made to decrease the percent lethality associated with the PRF mutant virus vaccination and the level of illness observed in the vaccinated mice, as well as potentially increasing the levels of neutralizing antibodies produced.

Overall, our findings suggest that attenuation of −1 PRF strongly reduced VEEV neuropathogenicity of the virus (as evidenced by decreased viral titers in the brain and increased survival) and provided protection when used as a vaccine thus unveiling a promising new avenue of inquiry toward the development of safe and effective live attenuated vaccines directed against VEEV and perhaps other −1 PRF-utilizing members of the *Togavirus* and *Flavivirus* families.

While the current study has many limitations to consider, such as the clinical illness and some instances of death associated with exposure to the mutant PRF virus, the results suggest that this strategy could be more effective if combined with other specific mutations to the virus. The PRF mutant virus only has 3 silent coding mutations that differentiate it from the WT TrD (as shown in Fig 1B). Furthermore, these silent coding changes are located on the wobble base of the codon and therefore it is possible that the mutant PRF virus reverted to WT virus at some point during our *in vivo* studies and could have contributed to the clinical symptoms and death observed in some animals. Future studies will incorporate the sequencing of the virus in the blood and organs collected prior to death in these animals to determine if reversion occurred. Ideally, live attenuated virus vaccine strains should be engineered to minimize the risk of reversion via back mutation. To minimize this possibility, the best strategy is to introduce multiple mutations targeting

different functional sections of the viral genome. We are currently exploring mutations of Termination codon readthrough (TCR) elements, which allow the production of the P1234 polyprotein as opposed to just the P123 polyprotein (Fig. 1B). The P1234 encodes for nsP1, nsP2, nsP3 and nsP4, thus enabling production of the critical RNA dependent RNA polymerase (nsP4) of the virus. We believe an ideal vaccine strain would be one harboring mutations in the TCR and the -1 PRF signal i.e. at two different genomic locations. More research into that aspect is ongoing in our lab and will serve to help us further understand and characterize the results presented here.

REFERENCES

1) Zacks MA, Paessler S. ENCEPHALITIC ALPHAVIRUSES. *Veterinary microbiology*. 2010;140(3-4):281. doi:10.1016/j.vetmic.2009.08.023.

2) Weaver S.C., Ferro C., Barrera R., Boshell J., Navarro J.C. Venezuelan equine encephalitis. Annu. Rev. Entomol. 2004;49:141–174. doi:10.1146/annurev.ento.49.061802.123422.

3) Lundberg L, Carey B, Kehn-Hall K. Venezuelan Equine Encephalitis Virus Capsid—The Clever Caper. *Viruses*. 2017;9(10):279. doi:10.3390/v9100279.

4) Ronca SE, Dineley KT, Paessler S. Neurological Sequelae Resulting from Encephalitic Alphavirus Infection. *Frontiers in Microbiology*. 2016;7:959.

5) Steele, K. E., and N. A. Twenhafel. "Review Paper." *Veterinary Pathology*, vol. 47, no. 5, 2010, pp. 790–805., doi:10.1177/0300985810372508.

6) Kielian M, Chanel-Vos C, Liao M. Alphavirus Entry and Membrane Fusion. *Viruses*. 2010;2(4):796-825. doi:10.3390/v2040796.

7) Li C, Guillén J, Rabah N, et al. mRNA Capping by Venezuelan Equine Encephalitis Virus nsP1: Functional Characterization and Implications for Antiviral Research. Diamond MS, ed. *Journal of Virology*. 2015;89(16):8292-8303. doi:10.1128/JVI.00599-15.

8) Kim DY, Atasheva S, Frolova EI, Frolov I. Venezuelan Equine Encephalitis Virus nsP2 Protein Regulates Packaging of the Viral Genome into Infectious Virions. *Journal of Virology*. 2013;87(8):4202-4213. doi:10.1128/JVI.03142-12.

9) Amaya M., Brooks-Faulconer T., Lark T., Keck F., Bailey C., Raman V., Narayanan A. Venezuelan equine encephalitis virus non-structural protein 3 (nsp3) interacts with RNA helicases ddx1 and ddx3 in infected cells. Antivir. Res. 2016;131:49–60. doi: 10.1016/j.antiviral.2016.04.008.

10) Kamer G, Argos P. Primary structural comparison of RNA-dependent polymerases from plant, animal and bacterial viruses. *Nucleic Acids Research*. 1984;12(18):7269-7282.

11) Jose J., Snyder J.E., Kuhn R.J. A structural and functional perspective of alphavirus replication and assembly. Future Microbiol. 2009;4:837–856. doi: 10.2217/fmb.09.59.

12) Ramsey J, Mukhopadhyay S. Disentangling the Frames, the State of Research on the Alphavirus 6K and TF Proteins. Kümmerer BM, Ahola T, eds. *Viruses*. 2017;9(8):228. doi:10.3390/v9080228.

13) Kendra JA, de la Fuente C, Brahms A, et al. Ablation of Programmed −1 Ribosomal Frameshifting in Venezuelan Equine Encephalitis Virus Results in Attenuated Neuropathogenicity. Dermody TS, ed. *Journal of Virology*. 2017;91(3):e01766-16. doi:10.1128/JVI.01766-16.

14) LeBlanc J, Weil J, Beemon K. Posttranscriptional regulation of retroviral gene expression: primary RNA transcripts play three roles as pre-mRNA, mRNA, and genomic RNA. *Wiley interdisciplinary reviews RNA*. 2013;4(5):10.1002/wrna.1179. doi:10.1002/wrna.1179.

15) Sanchez A, Trappier SG, Mahy BW, Peters CJ, Nichol ST. The virion glycoproteins of Ebola viruses are encoded in two reading frames and are expressed through transcriptional editing. *Proceedings of the National Academy of Sciences of the United States of America*. 1996;93(8):3602-3607.

16) Dinman JD. Programmed Ribosomal Frameshifting Goes Beyond Viruses: Organisms from all three kingdoms use frameshifting to regulate gene expression, perhaps signaling a paradigm shift. *Microbe (Washington, DC)*. 2006;1(11):521-527.

17) Jacobs JL, Belew AT, Rakauskaite R, Dinman JD. Identification of functional, endogenous programmed −1 ribosomal frameshift signals in the genome of *Saccharomyces cerevisiae*. *Nucleic Acids Research*. 2007;35(1):165-174. doi:10.1093/nar/gkl1033.

18) Moomau C, Musalgaonkar S, Khan YA, Jones JE, Dinman JD. Structural and Functional Characterization of Programmed Ribosomal Frameshift Signals in West Nile Virus Strains Reveals High Structural Plasticity Among *cis*-Acting RNA Elements. *The Journal of Biological Chemistry*. 2016;291(30):15788-15795. doi:10.1074/jbc.M116.735613.

19) Firth AE, Brierley I. 2012. Non-canonical translation in RNA viruses. J Gen Virol 93:1385–1409. https://doi.org/10.1099/vir.0.042499-0.

20) Snyder JE, Kulcsar KA, Schultz KLW, Riley CP, Neary JT, Marr S, Jose J, Griffin DE, Kuhn RJ. 2013. Functional characterization of the alphavirus TF protein. J Virol 87:8511– 8523. https://doi.org/10.1128/JVI.00449-13.

21) Dinman JD. Mechanisms and Implications of Programmed Translational Frameshifting. *Wiley interdisciplinary reviews RNA*. 2012;3(5):661-673. doi:10.1002/wrna.1126.

22) Dinman JD. Mechanisms and Implications of Programmed Translational Frameshifting. *Wiley interdisciplinary reviews RNA*. 2012;3(5):661-673. doi:10.1002/wrna.1126.

23) Chung BY-W, Firth AE, Atkins JF. 2010. Frameshifting in alphaviruses: a diversity of 3′ stimulatory structures. J Mol Biol 397:448–456. doi:10.1016/j.jmb.2010.01.044.

24) Belew AT, Hepler NL, Jacobs JL, Dinman JD. 2008. PRFdb: a database of computationally predicted eukaryotic programmed 1 ribosomal frameshift signals. BMC Genomics 9:339. https://doi.org/10.1186/1471 -2164-9-339.

25) Kinney RM, Chang GJ, Tsuchiya KR, et al. Attenuation of Venezuelan equine encephalitis virus strain TC-83 is encoded by the 5'-noncoding region and the E2 envelope glycoprotein. *Journal of Virology*. 1993;67(3):1269-1277.

26) Brierley I. 1995. Ribosomal frameshifting on viral RNAs. J Gen Virol 76:1885–1892. doi:10.1099/0022-1317-76-8-1885.

27) Davis NL, Willis LV, Smith JF, Johnston RE. 1989. In vitro synthesis of infectious Venezuelan equine encephalitis virus RNA from a cDNA clone: analysis of a viable deletion mutant. Virology 171:189–204. doi:10.1016/0042-6822(89)90526-6.

28) Melian EB, Hall-Mendelin S, Du F, Owens N, Bosco-Lauth AM, Nagasaki T, Rudd S, Brault AC, Bowen RA, Hall RA, van den Hurk AF, Khromykh AA. 2014. Programmed ribosomal frameshift alters expression of West Nile virus genes and facilitates virus replication in birds and mosquitoes. PLoS Pathog10:e1004447.

29) Melian EB, Hinzman E, Nagasaki T, Firth AE, Wills NM, Nouwens AS, Blitvich BJ, Leung J, Funk A, Atkins JF, Hall R, Khromykh AA. 2010. NS1′ of flaviviruses in the Japanese encephalitis virus serogroup is a product of ribosomal frameshifting and plays a role in viral neuroinvasiveness. J Virol 84:1641–1647. doi:10.1128/JVI.01979-09.

30) Taylor A, Melton JV, Herrero LJ, Thaa B, Karo-Astover L, Gage PW, Nelson MA, Sheng K-C, Lidbury BA, Ewart GD, McInerney GM, Merits A, Mahalingam S. 2016. Effects of an in-frame deletion of the *6k*gene locus from the genome of Ross River virus. J Virol 90:4150–4159. doi:10.1128/JVI.03192-15.

31) Kinney RM, Chang GJ, Tsuchiya KR, et al. Attenuation of Venezuelan equine encephalitis virus strain TC-83 is encoded by the 5'-noncoding region and the E2 envelope glycoprotein. *Journal of Virology*. 1993;67(3):1269-1277.

32) Paessler S, Weaver SC. Vaccines for Venezuelan equine encephalitis. *Vaccine*. 2009;27S4:D80-D85. doi:10.1016/j.vaccine.2009.07.095.

33) Berge TO, Banks IS, Tigertt WD. 1961. Attenuation of Venezuelan equine encephalomyelitis virus by in vitro cultivation in guinea pig heart cells. Am J Hyg (Lond) 73:209–218.

34) Johnson BJB, Kinney RM, Kost CL, Trent DW. 1986. Molecular determinants of alphavirus neurovirulence: nucleotide and deduced protein sequence changes during attenuation of Venezuelan equine encephalitis virus. J Gen Virol 67:1951–1960. doi:10.1099/0022-1317-67-9-1951.

35) Bernard KA, Klimstra WB, Johnston RE. 2000. Mutations in the E2 glycoprotein of Venezuelan equine encephalitis virus confer heparan sulfate interaction, low morbidity, and rapid clearance from blood of mice. Virology 276:93–103. doi:10.1006/viro.2000.0546.

36) Davis NL, Willis LV, Smith JF, Johnston RE. 1989. In vitro synthesis of infectious Venezuelan equine encephalitis virus RNA from a cDNA clone: analysis of a viable deletion mutant. Virology 171:189–204. doi:10.1016/0042-6822(89)90526-6.

37) National Research Council. 2011. Guide for the care and use of laboratory animals, 8th ed National Academies Press, Washington, DC.

38) Melian EB, Hinzman E, Nagasaki T, Firth AE, Wills NM, Nouwens AS, Blitvich BJ, Leung J, Funk A, Atkins JF, Hall R, Khromykh AA. 2010. NS1′ of flaviviruses in the Japanese encephalitis virus serogroup is a product of ribosomal frameshifting and plays a role in viral neuroinvasiveness. J Virol 84:1641–1647. doi:10.1128/JVI.01979-09.

39) Taylor A, Melton JV, Herrero LJ, Thaa B, Karo-Astover L, Gage PW, Nelson MA, Sheng K-C, Lidbury BA, Ewart GD, McInerney GM, Merits A, Mahalingam S. 2016. Effects of an in-frame deletion of the *6k*gene locus from the genome of Ross River virus. J Virol 90:4150–4159. doi:10.1128/JVI.03192-15.

40) Hallengärd D, Kakoulidou M, Lulla A, et al. Novel Attenuated Chikungunya Vaccine Candidates Elicit Protective Immunity in C57BL/6 mice. *Journal of Virology*. 2014;88(5):2858-2866. doi:10.1128/JVI.03453-13.

41) Martin SS, Bakken RR, Lind CM, et al. Telemetric analysis to detect febrile responses in mice following vaccination with a live-attenuated virus vaccine. *Vaccine*. 2009;27(49):6814-6823. doi:10.1016/j.vaccine.2009.09.013.

42) Taylor KG, Paessler S. Pathogenesis of Venezuelan equine encephalitis. Vet Microbiol. 2013 Nov 29;167(1-2):145-50. doi: 10.1016/j.vetmic.2013.07.012.

43) Jackson SJ, Andrews N, Ball D, et al. Does age matter? The impact of rodent age on study outcomes. *Laboratory Animals*. 2017;51(2):160-169. doi:10.1177/0023677216653984.

44) Jacks T. 1990. Translational suppression in gene expression in retroviruses and retrotransposons. Curr Top Microbiol Immunol 157:93–124.

45) Sheju-Shilaga M, Crowe SM, Mak J. 2001. Maintenance of the Gag/Gag-Pol ratio is important for human immunodeficiency virus type 1 RNA dimerization and viral infectivity. J Virol 75:1834–1841. doi:10.1128/JVI.75.4.1834-1841.2001.

46) Dinman JD, Wickner RB. 1992. Ribosomal frameshifting efficiency and Gag/Gag-Pol ratio are critical for yeast M1 double-stranded RNA virus propagation. J Virol 66:3669–3676.

47) Dinman JD, Ruiz-Echevarria MJ, Peltz SW. 1998. Translating old drugs into new treatments: identifying compounds that modulate programmed −1 ribosomal frameshifting and function as potential antiviral agents. Trends Biotechnol 16:190–196. doi:10.1016/S0167-7799(97)01167-0.

48) Barry JK, Miller WA. 2002. A −1 ribosomal frameshift element that requires base pairing across four kilobases suggests a mechanism of regulating ribosome and replicase traffic on a viral RNA. Proc Natl Acad Sci USA 99:11133–11138. doi:10.1073/pnas.162223099.

49) Brierley I, Dos Ramos FJ. 2005. Programmed ribosomal frameshifting in HIV-1 and the SARS-CoV. Virus Res 119:23–42.

50) Plant EP, Dinman JD. 2008. The role of programmed −1 ribosomal frameshifting in coronavirus propagation. Front Biosci 13:4873–4881.

51) Plant EP, Rakauskaite R, Taylor DR, Dinman JD. 2010. Achieving a golden mean: mechanisms by which coronaviruses ensure synthesis of the correct stoichiometric ratios of viral proteins. J Virol 84:4330–4340. doi:10.1128/JVI.02480-09.

52) Moomau C, Musalgaonkar S, Khan YA, Jones JE, Dinman JD. 2016. Structural and functional characterization of programmed ribosomal frameshift signals in West Nile virus strains reveals high structural plasticity among cis-acting RNA elements. J Biol Chem 291:15788–15795. doi:10.1074/jbc.M116.735613.

53) Young LB, Melian EB, Khromykh AA. 2013. NS1′ colocalizes with NS1 and can substitute for NS1 in West Nile virus replication. J Virol 87:9384–9390. doi:10.1128/JVI.01101-13.

54) Winkelmann ER, Widman DG, Suzuki R, Mason PW. 2011. Analyses of mutations selected by passaging a chimeric flavivirus identify mutations that alter infectivity and reveal an interaction between the structural proteins and the nonstructural glycoprotein NS1. Virology 421:96–104. doi:10.1016/j.virol.2011.09.007.

55) Advani VM, Dinman JD. 2016. Reprogramming the genetic code: the emerging role of ribosomal frameshifting in regulating cellular gene expression. Bioessays 38:21–26. doi:10.1002/bies.201500131.

56) Mukhopadhyay S, Zhang W, Gabler S, Chipman PR, Strauss EG, Strauss JH, Baker TS, Kuhn RJ, Rossmann MG. 2006. Mapping the structure and function of the E1 and E2 glycoproteins in alphaviruses. Structure 14:63–73. doi:10.1016/j.str.2005.07.025.

57) Pedersen CE, Robinson DM, Cole FE. 1972. Isolation of the vaccine strain of Venezuelan equine encephalomyelitis virus from mosquitoes in Louisiana. Am J Epidemiol 95:490–496.

58) Pittman PR, Makuch RS, Mangiafico JA, Cannon TL, Gibbs PH, Peters CJ. 1996. Long-term duration of detectable neutralizing antibodies after administration of live-attenuated VEE vaccine and following booster vaccination with inactivated VEE vaccine. Vaccine 14:337–343. doi:10.1016/0264-410X(95)00168-Z.

59) Paessler S, Weaver SC. 2009. Vaccines for Venezuelan equine encephalitis. Vaccine 27(Suppl 4):D80–D85. doi:10.1016/j.vaccine.2009.07.095.

BIOGRAPHY

Caitlin Woodson Lehman was born in Lynchburg Virginia and graduated from Brookville High School, Lynchburg, Virginia, in 2006. She received her Bachelor of Science from Virginia Tech in 2010. After working as the Animal Facility Supervisor at the National Center for Biodefense and Infectious Diseases since 2014, she decided she wanted to understand and study the *in vitro* research that goes into *in vivo* research so starting in Fall semester 2016 she pursued her Masters in Biology at George Mason University with a concentration in Microbiology and Infectious Diseases. Following graduation, she intends to stay at George Mason University as a Research Associate to pursue her Ph.D. in Biosciences.